THE EFFECTS OF CHLORIDES, HYDROGEN CHLORIDE, AND SULFUR DIOXIDE IN THE OXIDATION OF STEELS BELOW DEPOSITS

H. J. GRABKE, E. REESE and M. SPIEGEL

Max-Planck-Institut für Eisenforschung GmbH, P.O. Box 140444, D-40074 Düsseldorf, Germany

Abstract—Thermogravimetric studies have been conducted on the oxidation of a low alloy steel at 500°C and high alloy steels at 600 and 700°C in which either NaCl or a fly ash (from a waste incineration plant) was deposited on the scale of the steels after 24 h pre-oxidation. The chlorides in the deposits react with the scale under formation of chlorine which enters the scale and causes accelerated oxidation, by the formation of $FeCl_2(s)$ at the scale/metal interface, evaporation of $FeCl_2(g)$ and its oxidation to Fe_2O_3 at the scale surface; chlorine partially returning into the scale. This leads to a porous unprotective scale and active oxidation, catalysed by chlorine. By variation of several parameters it was shown that the evaporation of $FeCl_2(g)$ and its outward diffusion through the scale is the rate controlling step of the active oxidation. The presence of SO_2 in the atmosphere causes a minor increase of active corrosion by the sulfation of chlorides and the generation of chlorine. The presence of HCl in the atmosphere causes a transformation of sulfates in the deposits into chlorides, which induce enhanced active oxidation. In the presence of balanced concentrations of HCl and SO_2 in the atmosphere, however, the corrosion is limited.

INTRODUCTION

The high temperature corrosion of steels by chlorine and chlorides plays a detrimental role in power plants where municipal waste or coal containing chlorides are used as a fuel. In the incineration atmospheres of such plants, rapid wastage is observed in the heat exchanger tubes which are generally made of low alloy steels. The tubes are covered with thick layers of deposits, formed by deposition of fly ash on the oxide scale of the steel surface. In failure cases a layer of the condensed chloride $FeCl_2$ has been observed at the metal/oxide interface and the oxide layer above the chloride precipitates was very porous and loose, i.e. it could not serve as a protective layer.[1]

The effects of HCl and chlorides on the high temperature oxidation of iron and steels have been previously studied.[2–6] The most striking effect in these studies is the rapid response of the corrosion phenomena on the introduction of the chlorine containing contamination into the environment. As soon as sodium chloride is introduced, as a vapour into the oxidizing atmosphere or as a grain on to the oxide scale of a steel,[2,3] the oxidation is strongly accelerated. A vibrational technique indicated that the main effect is considerable damage to the oxide scale.[2] In a hot stage microscope blistering and cracking of the oxide scale was observed upon depositing sodium chloride on the sample.[3] In thermogravimetric studies an immediate acceleration of the oxidation rate was observed upon introduction of HCl into the gas flow (see Fig. 1) or upon deposition of some sodium chloride on to the pre-oxidized sample.[5,6] After introduction of the chlorine containing contamination, the
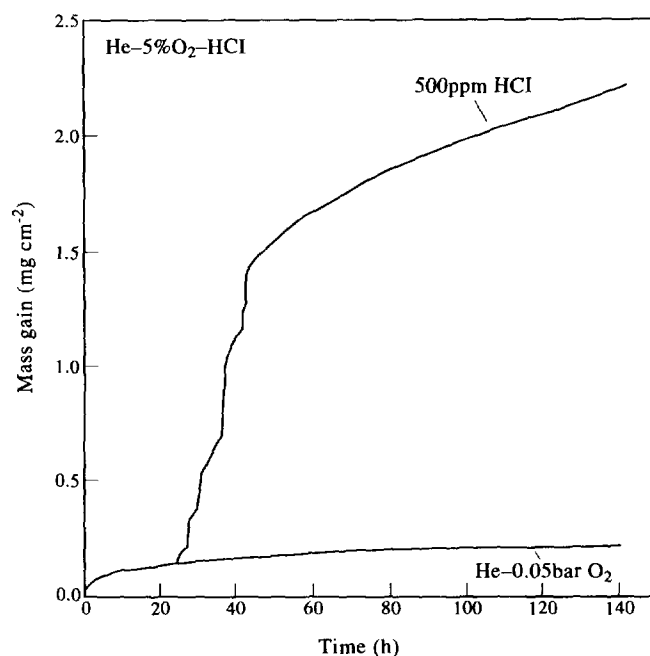
Fig. 1.   Mass gain of the $2\frac{1}{4}Cr-1Mo$-steel at 500°C in He–O_2 and in He–O_2–500 vppmHCl after pre-oxidation for 24 h.

oxide scale is not adherent and protective, but very loose, cracked and porous (see Fig. 2). Since in this state there is no passivation by a protective oxide layer, the oxidation in the presence of chlorine containing contaminants has been named active oxidation, i.e. the oxidation of steel accelerated by the presence of chlorine.[7,8] Under certain conditions, metals, e.g. Ni, even ignite in oxidizing–chlorinating atmospheres.[9] The mechanism and kinetics of the active oxidation of a low alloy steel will be described later. It will be demonstrated that a reaction circuit occurs between oxide/metal interface and scale surface which is catalysed by chlorine. One aim of the studies was to find the rate controlling step of this circuit, in order to develop ways and means to retard and suppress the process of active oxidation. The role of the chlorides and the active oxidation in the corrosion beneath fly ash deposits was to be elucidated, and how the corrosion is affected by the presence of SO_2 and HCl in the atmosphere.

EXPERIMENTAL METHOD

The studies on high temperature corrosion by chlorides[5,6] and by fly ash deposits[10] were conducted in a flow apparatus combined with a thermobalance (Fig. 3). The flow apparatus served for the cleaning and dosing of the gases He, O_2, SO_2 and HCl by capillary flow meters. The thermobalance had a horizontal specimen holder so that solid salts or fly ash could be deposited on the surface of the steel. The steel specimens of size $20 \times 10 \times 2$ mm³ were ground with SiC, polished with a diamond paste and cleaned in acetone. Generally, the specimens were pre-oxidized in He–O_2 and then the salt or fly ash was deposited on to the scale of the upper side of the specimen. This could be performed *in-situ* during an experiment at the reaction temperature,[5,6] but in most cases the experiment was interrupted to distribute the deposit evenly onto the sample.[10]
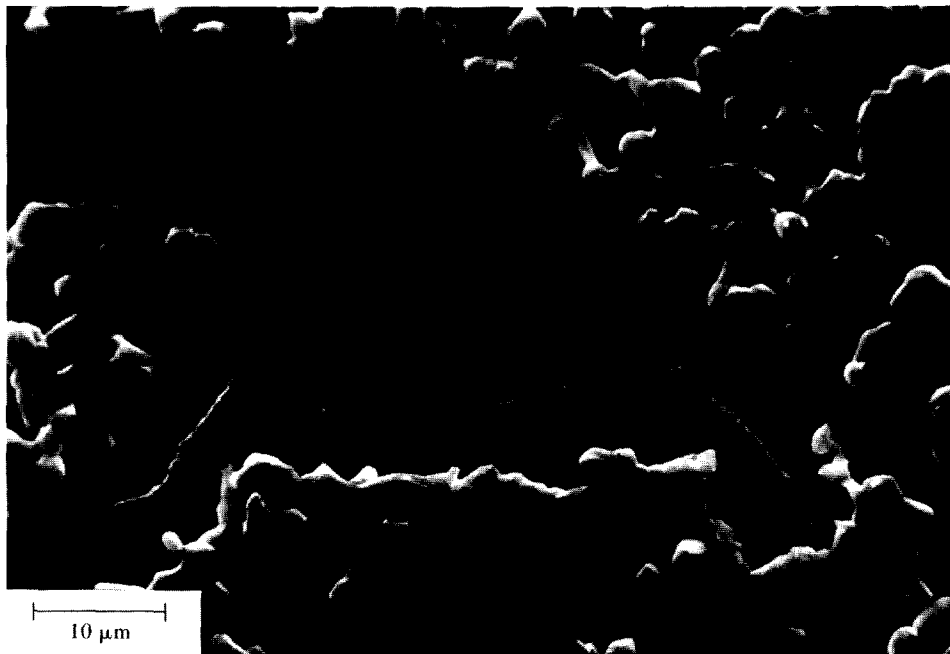
Fig. 2.   Morphology of an oxide scale on the $2\frac{1}{4}$Cr–1Mo-steel after active oxidation. SEM photo, top view.
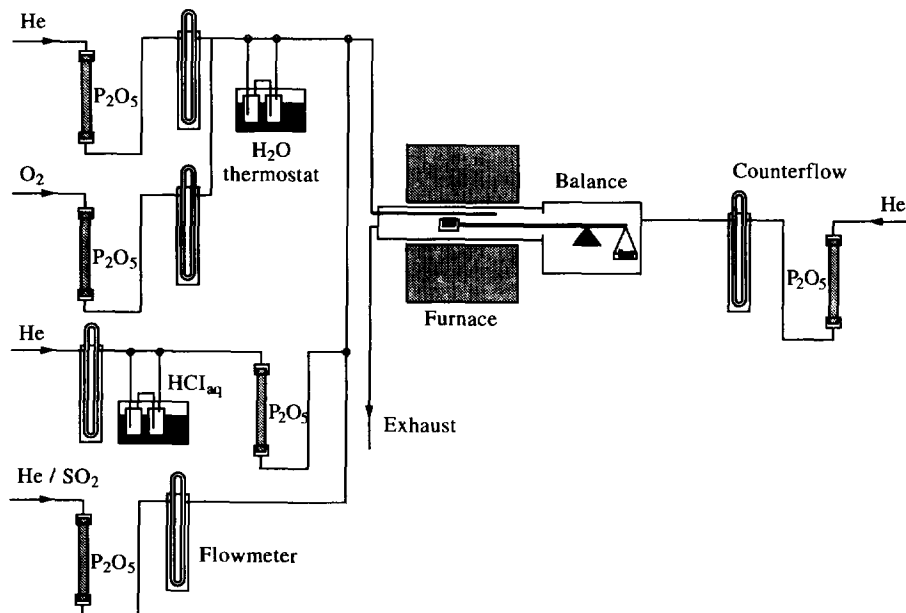

Fig. 3.   Schematics of the experimental set up for thermogravimetric experiments with deposits on the sample, flow apparatus for cleaning and dosing the gases and horizontal balance.

Table 1.   Compositions of the investigated steels (in wt%)

$2\frac{1}{4}$Cr–1Mo	2.21 Cr, 0.91 Mo, 0.43 Mn, 0.1 C
12CrMoV	11.9 Cr, 1.27 Mo, 0.32 V, 0.18 C
20Cr–12Ni	19.8 Cr, 11.2 Ni, 1.76 Si, 0.7 C
25Cr–20Ni	25.6 Cr, 20.5 Ni, 1.85 Si, 0.1 Nb, 0.45 C

Table 2.   Phases in the fly ash deposit

$Ca_2MgSi_2O_7$ Akermanit
$(K,Na)_2Ca_2(SO_4)_3$ Langbeinit
K_2SO_4, $CaSO_4$, $(K, Na)Cl$

Helium was used as a carrier gas, since this allows a very sensitive measurement free of vibrations and disturbances[11] and 0.05 or 0.13 bar O_2 was added. The SO_2-addition was made by a flow of He–1%SO_2. The HCl was added by saturating a partial flow of He in hydrochloric acid at a controlled temperature and subsequent removal of the water vapour by phosphor pentoxide. The gas mixtures, He–O_2, He–O_2–SO_2, He–O_2–HCl or He–O_2–SO_2–HCl, were introduced into the reaction chamber of the thermobalance through a capillary; the thermobalance itself was flushed and protected by a counterflow of He (see Fig. 3).
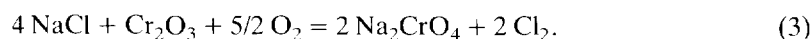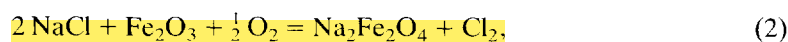
The compositions of the steels investigated are given in Table 1. The phases found in the fly ash used, which was obtained from a waste incineration plant, are listed in Table 2. The fly ash consists mainly of spherical hollow silicate particles covered with sulfates and chlorides (Fig. 4), which condense on these glass balls during cooling and deposition. This kind of distribution, offering a high surface area in such deposits, renders the sulfates and chlorides rather reactive for transformations by reactions with the gas atmosphere.

MECHANISM OF THE ACTIVE OXIDATION

The mechanism of the active oxidation can be understood on the basis of some thermodynamic fundamentals and some experimental observations. First, chlorine can be formed from the oxidation of HCl, catalysed by the oxides (Weldon process) of the scale:

$$2\,HCl + \tfrac{1}{2}O_2 = Cl_2 + H_2O, \tag{1}$$

or from the reaction of condensed chlorides, such as NaCl with oxides of the scale, e.g.

$$2\,NaCl + Fe_2O_3 + \tfrac{1}{2}O_2 = Na_2Fe_2O_4 + Cl_2, \tag{2}$$

$$4\,NaCl + Cr_2O_3 + 5/2\,O_2 = 2\,Na_2CrO_4 + 2\,Cl_2. \tag{3}$$

Equilibrium chlorine pressures for such Cl_2 generating reactions are in the range 10^{-10}–10^{-13} bar Cl_2.[1] If the chlorine can penetrate the oxide scale, chlorides of iron and the alloying elements can be formed at the scale/metal interface, since the oxygen pressure is low at this interface (see Fig. 5) and their formation pressure is exceeded, e.g. according to the reaction

$$Fe + Cl_2 = FeCl_2(s). \tag{4}$$

The metal chlorides at this interface have a considerable vapour pressure—for $FeCl_2(s)$ at 500°C it is $4 \cdot 10^{-5}$ bar—thus, a continuous evaporation will take place,
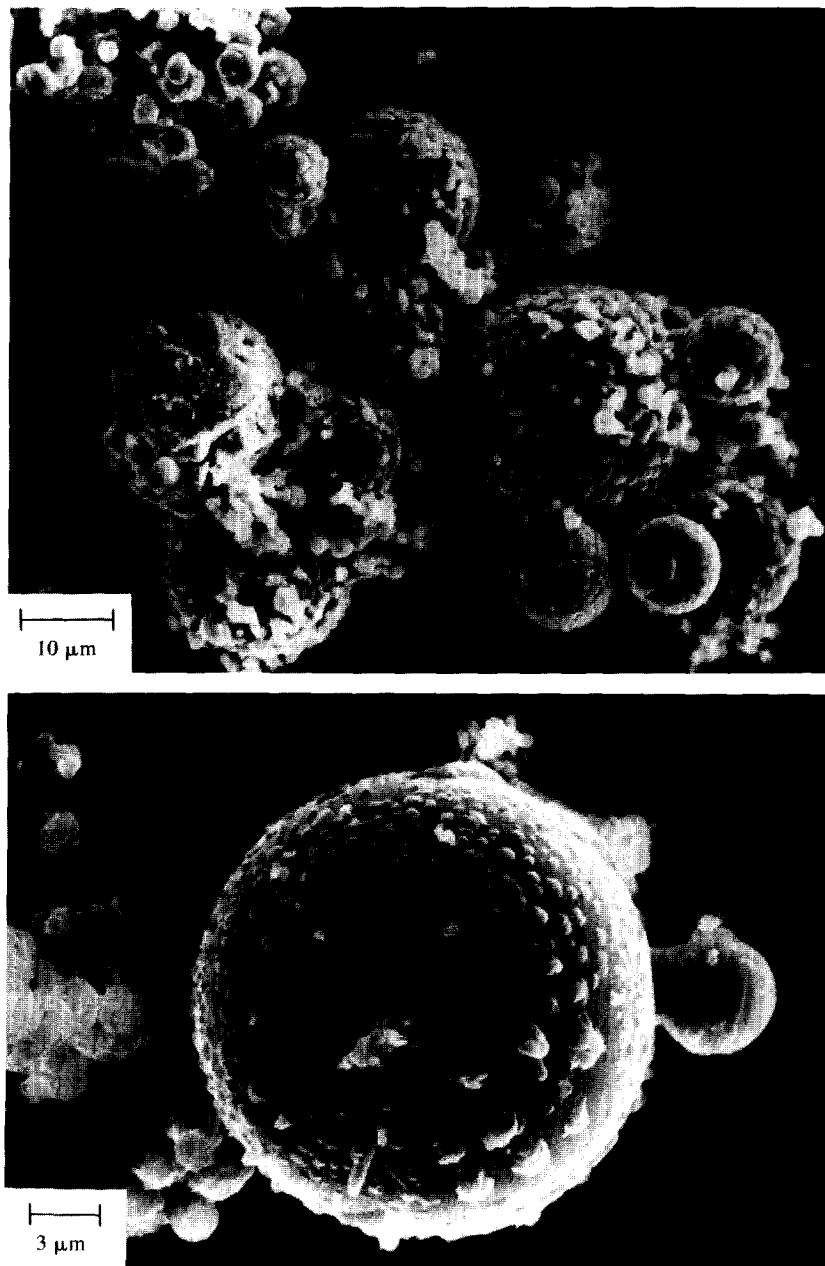
Fig. 4.   SEM micrograph of the fly ash deposits—silicate spheres covered with sulfates and chlorides.

$$FeCl_2(s) = FeCl_2(g), \tag{5}$$

and the volatile chloride will diffuse outward through cracks and pores of the scale. On its way outward, regions of higher oxygen pressure are reached where the chloride is oxidized to Fe_3O_4 and/or Fe_2O_3:
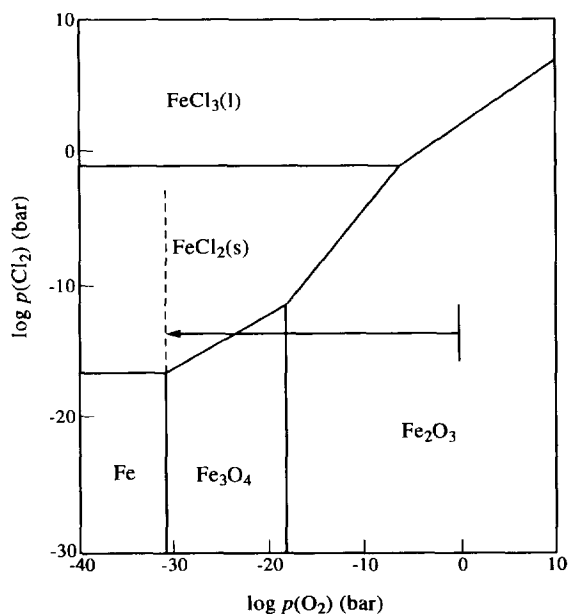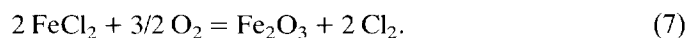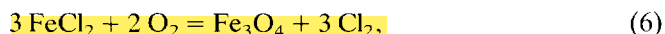
Fig. 5. Phase stability diagram of the system Fe–O–Cl at 500°C—at the pO_2 corresponding to the Fe/Fe_3O_4 phase boundary, $FeCl_2(s)$ is stable.

$$3\,FeCl_2 + 2\,O_2 = Fe_3O_4 + 3\,Cl_2, \tag{6}$$

$$2\,FeCl_2 + 3/2\,O_2 = Fe_2O_3 + 2\,Cl_2. \tag{7}$$

The reactions (1) or (2), (4), (5) and (7) comprise the main reaction path in the active corrosion of iron and low alloy steels (Fig. 6), as proven by the observations: (i) of ferrates formed by interaction of solid alkali chlorides and scales on steels, (ii) of the formation of solid metal chlorides, mainly $FeCl_2(g)$ at the oxide/metal interface and (iii) of the appearance of the scales after some time of active oxidation. Fe_2O_3 is mainly observed in crystalline structures as they are typical for products of chemical transport reactions (Fig. 2). The scale is virtually detached from the substrate, its adherence to the steel surface is minute and, thus, the Fe_2O_3 phase can be stable.

For high alloy steels the reaction path is similar. The chlorine stems from the reactions of HCl or chlorides with $FeCr_2O_4$ or Cr_2O_3, according to reaction (3). As for the subsequent reactions, reactions (4), (5) and (7) again prevail. Mainly $FeCl_2$ is formed, because its vapour pressure is highest (compared to $NiCl_2$, $CoCl_2$, $CrCl_2$ and $CrCl_3$).[1] At high corrosion temperatures no solid chlorides of Fe and the alloying elements can be found at the oxide/metal interface, since the volatile species are formed immediately. In one failure case only traces of the responsible element, i.e. Cl, might be detected.[12]

In this mechanism of active corrosion, one step is still not fully elucidated, i.e. the penetration of chlorine from reactions (1), (2), (3), etc., through the oxide scale. It has been mentioned already that the active oxidation starts with nearly no incubation time after introduction of HCl or deposition of chlorides on the scale. Thus, solid state diffusion and, also, grain boundary diffusion can be excluded for the transport of chlorine to the interface. Even molecular diffusion through cracks and pores of the

| Gas | | Fe_2O_3 | | Fe_3O_4 | | Metal |

$$2\ NaCl\ +\ Fe_2O_3\ +\ 1/2\ O_2$$
$$=\ Na_2Fe_2O_4 + Cl_2 \longrightarrow$$

$$Cl_2\ +\ Fe\ =\ FeCl_2(s)$$

$$FeCl_2(g)\ =\ FeCl_2(s)$$

$$3/2\ O_2\ +\ 2FeCl_2(g)$$
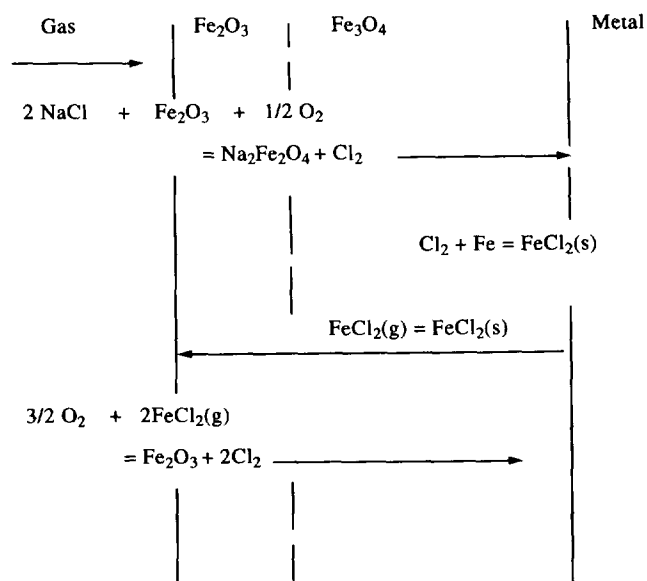$$=\ Fe_2O_3 + 2Cl_2 \longrightarrow$$

Fig. 6. Schematics of the reaction circuit of active oxidation.

scale cannot bring about the transport necessary to explain the abrupt increase of oxidation rate (Fig. 1). Somehow the chlorine itself must effect the creation of fast diffusion paths, possibly through grooves and fissures at grain boundaries. Such an effect has been observed in the growth of magnetite in steam at 200–300°C under the influence of chlorides.[13] For the high temperature oxidation, such effect of chlorine, however, has not been clearly proven due to the fast loosening and disintegration of the oxide scale.

THE KINETICS OF ACTIVE OXIDATION OF A LOW ALLOY STEEL

The kinetics of active oxidation were investigated in detail on a $2\frac{1}{4}$Cr–1Mo-steel,[5] the samples were always pre-oxidized in He–0.13 bar O_2, in most cases for 24 h, and then the active oxidation was started by depositing NaCl as a powder on to the oxide scale.

The temperature dependence was studied by experiments at 450, 550, 600 and 650°C (Fig. 7(a)). A logarithmic plot of the rates (after 100 h) vs $1/T$ yields an activation energy of 90 kJ mol^{-1}, which closely corresponds to the enthalpy of $FeCl_2$-evaporation. The variation of the pre-oxidation times 4, 24 and 96 h, leads to different oxide layer thicknesses at the start of active oxidation. The higher the pre-oxidation time and the thickness, the smaller was the initial acceleration (Fig. 7(b)). The rate is inversely proportional to the thickness of the scale. Variation of the area covered with NaCl showed that the rate of active oxidation is proportional to that area (Fig. 7(c)), whereas the variation of the amount of NaCl at constant area did not affect the rate.

The rate of active oxidation is nearly independent of the gas flow rate. A small decrease was observed with increasing flow rate.[5] This effect can be ascribed to the more effective removal of Cl_2 from the reaction circuit with increasing gas flow. The
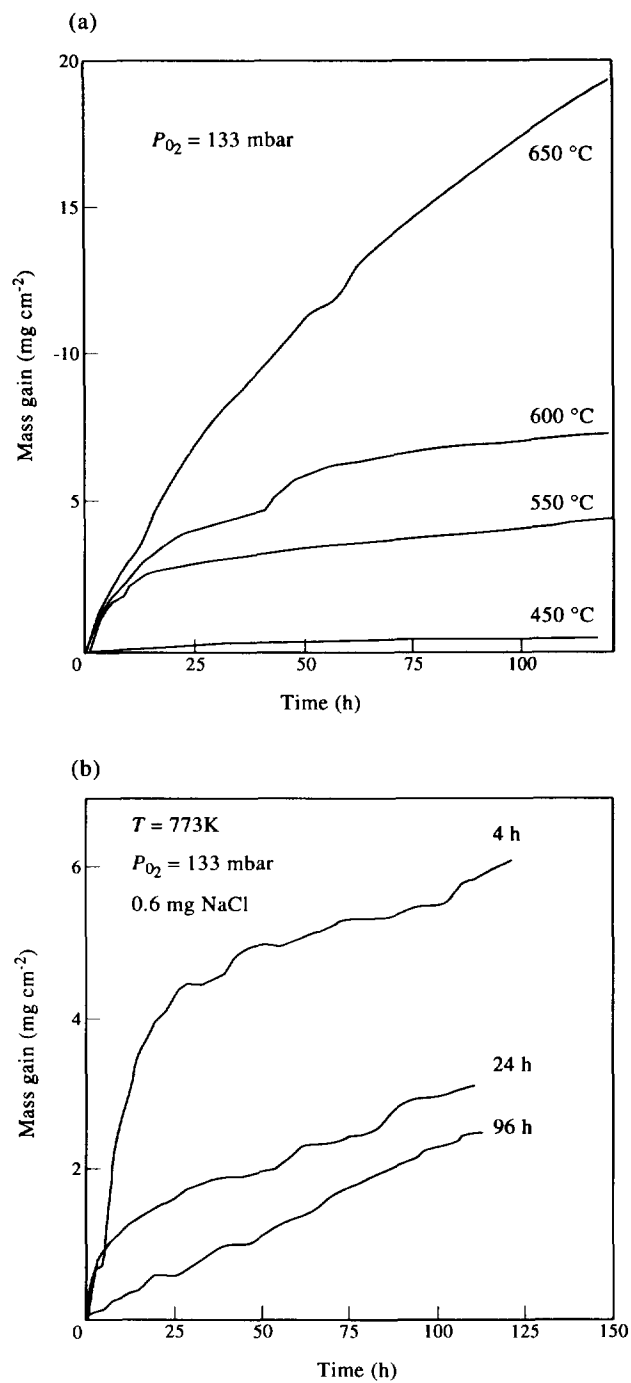
H. J. Grabke *et al.*

(a)

(b)

Fig. 7. Kinetics of the chloride induced active oxidation of the $2\frac{1}{4}$Cr–1Mo-steel at 500°C. (a) Mass gain vs time after pre-oxidation and addition of NaCl at different temperatures; (b) mass gain vs time after different pre-oxidation times, i.e. for different scale thicknesses (after 4 h: 0.04 mm, 24 h: 0.09 mm, 96 h: 0.19 mm); (c) mass gain vs time, after pre-oxidation and spreading of NaCl on different area sizes of the specimen.
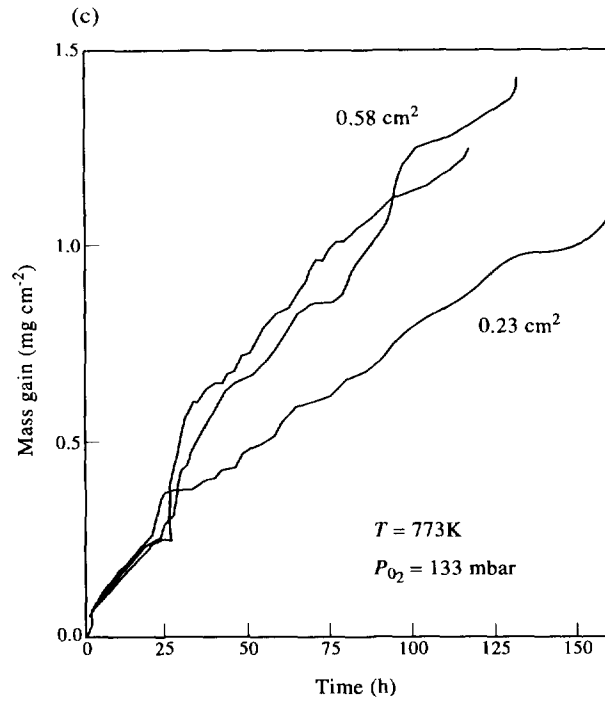
(c)

Fig. 7.   Contd.

rate varies only to a small extent if the equilibrium chlorine pressure at the oxide surface is varied. According to reaction equation (2) the chlorine pressure is proportional to $pO_2^{1/2}$; the dependence of the oxidation rate of pO_2 is much less.[5] The chlorine pressure can also be varied by the addition of SO_2. According to the reaction equation

$$2\,NaCl + SO_2 + O_2 = Na_2SO_4 + Cl_2, \tag{8}$$
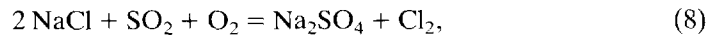
the chlorine pressure in equilibrium is proportional to pSO_2. The effect of pSO_2 on the oxidation rate is much less.[5] It can be concluded that the amount of Cl_2 available is not decisive, since the accessible interfacial area beneath the surface area covered with NaCl is also covered with $FeCl_2(s)$. The rate of $FeCl_2(g)$ outward diffusion through the oxide scale is rate controlling for the overall process of active oxidation. This is in agreement with the temperature dependence and the inverse dependence on the oxide thickness. The rate would correspond to the outward diffusion flow of $FeCl_2(g)$ through the open spaces in the oxide scales, pores, fissures and/or cracks, whatsoever. The diffusional flow is given by

$$j(FeCl_2) = \varepsilon \cdot \frac{D(FeCl_2)}{d}(p'(FeCl_2) - p''(FeCl_2)),$$

where ε is a labyrinth factor, resulting from the open space free for outward $FeCl_2$ diffusion, $D(FeCl_2)$ is the diffusivity of $FeCl_2(g)$ and $p(FeCl_2)$ its partial pressure at the interior interface $'$ and at the surface $''$. The latter value will be virtually zero so that one obtains

$$2\frac{dn(Fe_2O_3)}{A\,dt} = j(FeCl_2) = \varepsilon\,\frac{D(FeCl_2)}{d}\cdot p'(FeCl_2).$$

The rate of Fe_2O_3 formation (per unit area) is given by the outward flux of $FeCl_2$.

The temperature dependence mainly results from the temperature dependence of $p'(FeCl_2)$ which is the vapour pressure of $FeCl_2(s)$. The temperature dependence of the diffusivity of $FeCl_2(g)$, i.e. of a volatile species in the gas phase, is negligible $(\sim T^{1/2})$. The experimental result that the activation energy of active oxidation is similar to the enthalpy of $FeCl_2$-evaporation is sensible. This result, and the inverse proportionality of oxidation rate to $1/d$, confirm the rate control by outward diffusion of $FeCl_2(g)$ through a porous oxide scale. The value of ε can be assessed using experimental data for the formation rate of Fe_2O_3 in the active oxidation for a certain oxide thickness and approximate values for the diffusivity and saturation pressure of $FeCl_2(g)$. The result $\varepsilon \sim 10^{-5}$ indicates that the free space through which $FeCl_2(g)$ can diffuse outwards is in fact rather small, in spite of the loose and cracked appearance of the scale after active oxidation. It must, however, be taken into account that the ways for the outward diffusion of $FeCl_2(g)$ are blocked self acting by its reaction to Fe_2O_3, otherwise the rate of oxidation could be much higher. The knowledge of the rate-controlling step allows a discussion on ways and means to retard the active oxidation.

It may be noted that the chlorination of many metals in non-oxidizing atmospheres in many cases[15–18] is also governed by the evaporation by the volatile chloride from the solid chloride layer on the metal and controlled by the diffusion through the stagnant diffusion boundary layer into the flowing gas atmosphere.

THE CORROSION OF THE LOW ALLOY STEEL BENEATH DEPOSITS

In these experiments[10] the samples were also pre-oxidized for 24 h and then a certain amount of deposit was placed on the oxide scale. An immediate acceleration of the mass increase was observed, but the rate of mass gain levels off until after about 100 h when it is nearly equal to the rate without deposits (Fig. 8). Investigation of the samples after the experiment clearly showed that active oxidation had taken place. Beneath a loose, badly adherent oxide scale $FeCl_2$ was observed locally and the deposits were overgrown by Fe_2O_3. The chlorine which catalysed the active oxidation stems from the reaction of the mixed chlorides $(K,Na)Cl$ in the deposits with the Fe_2O_3 in the oxide scale. Since only the $(K,Na)Cl$ which is in direct contact with the scale can react in this solid state reaction, the chlorine formed will be lost after some time and the reaction fades away. The experiments are not very reproducible, since the amount of $(K,Na)Cl$ in the deposit which is in contact with the scale will vary from experiment to experiment.

The effect of sulfur dioxide SO_2 on the system deposit/scale/steel sample had to be investigated in two kinds of thermogravimetric experiments: first the interaction of $He–O_2–SO_2$ with the deposit was studied, then the interaction with the whole system of deposit, scale and steel.

The exposure of only deposits to the atmospheres with different SO_2 partial pressures already shows a mass increase, which is somewhat enhanced with increasing pSO_2 (Fig. 9(a)).

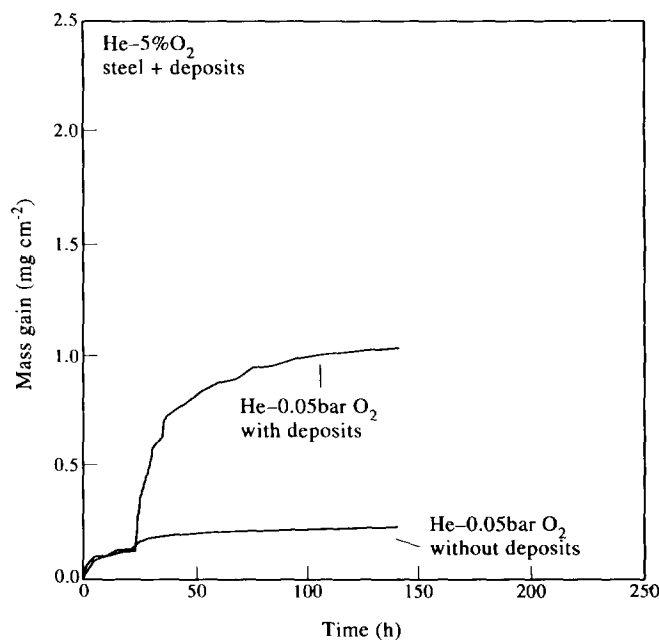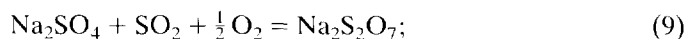The interactions of SO_2 and deposits led to the formation of pyrosulfates, which

Fig. 8.   Mass gain of the $2\frac{1}{4}$Cr–1Mo-steel after pre-oxidation in He–O_2 at 500°C without and with fly ash deposits, put on after 24 h.

were detected in the deposits after these experiments. The pyrosulfates form by the reaction

$$Na_2SO_4 + SO_2 + \tfrac{1}{2} O_2 = Na_2S_2O_7; \tag{9}$$

they are liquid at reaction temperature. If the melt of Na- and K-pyrosulfates reaches the scale, it will be converted to a complex sulfate,

$$3 Na_2S_2O_7(l) + Fe_2O_3 = 2 Na_3Fe(SO_4)_3, \tag{10}$$
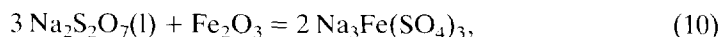
which was detected after the experiments. Such reaction certainly destroys the oxide scale on the steel. The formation of the pyrosulfates according to reaction (9) causes the mass increase. But also the conversion of chlorides into sulfates occurs:

$$2 (K,Na)Cl + SO_2 + \tfrac{1}{2}O_2 = (K,Na)_2SO_4 + Cl_2. \tag{11}$$
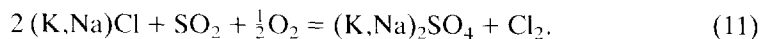
The latter reaction liberates some chlorine, but mainly near the surface of the deposits. So, most of this chlorine is lost to the atmosphere, but a small part will diffuse inward again.

The effect of hydrogen chloride HCl on the system deposit/scale/steel sample had at first to be investigated by studying the interaction of He–O_2–HCl and deposit separately. In such experiments a considerable decrease of mass was observed (Fig. 10(a)). By contrast, the mass gain by corrosion is strongly enhanced by the presence of HCl (Fig. 10(b)), after the experiment $FeCl_2$ was found beneath a loose oxide layer, which indicates active oxidation. The mass change of the deposit can be explained by the reaction of HCl with the mixed sulfate in the deposit

H. J. Grabke *et al.*

(a)

(b)
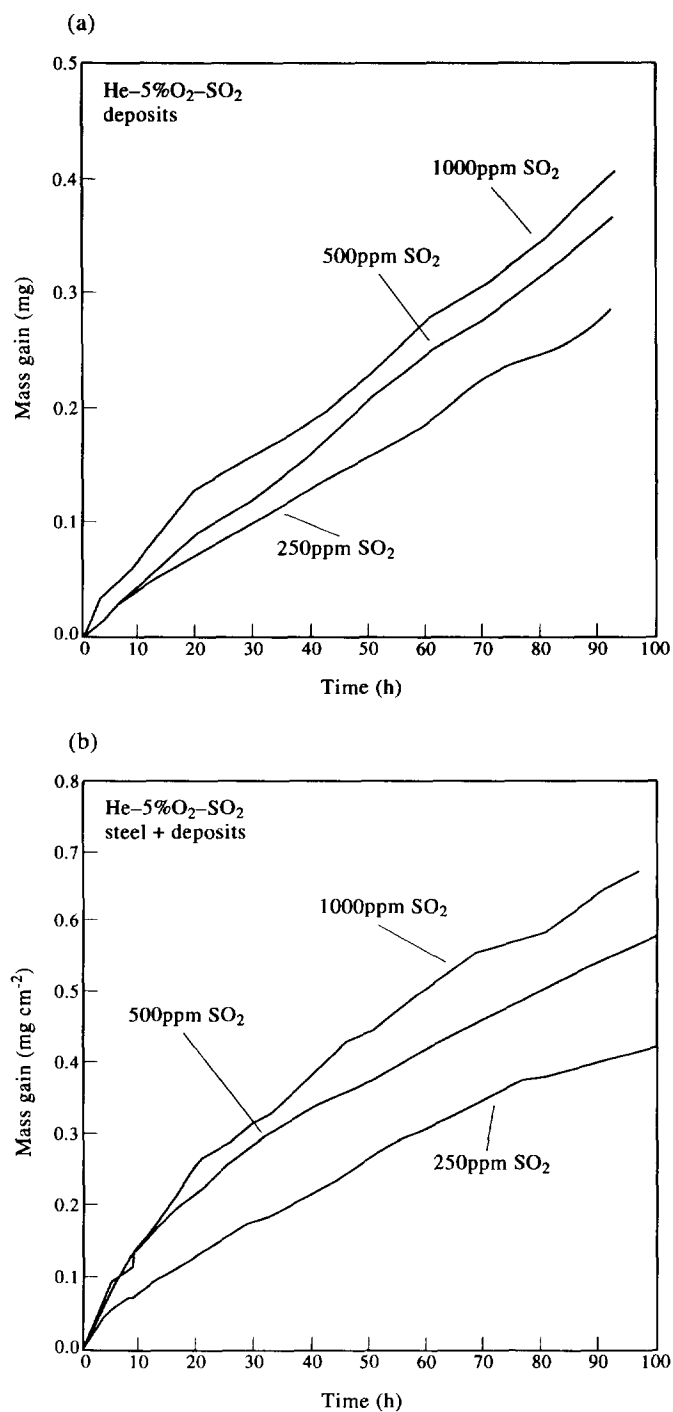
Fig. 9. Effects of SO_2 on the mass gain at 500°C: (a) of only the fly ash deposit by pyrosulfate formation (reaction (9)); (b) of the steel sample with fly ash deposit by sulfation (reaction (10)) and enhanced active corrosion; (c) differentiation of both effects, on deposit and on steel sample.
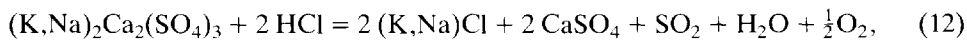
(c)

Fig. 9. Contd.

$$(K,Na)_2Ca_2(SO_4)_3 + 2 HCl = 2 (K,Na)Cl + 2 CaSO_4 + SO_2 + H_2O + \tfrac{1}{2}O_2, \qquad (12)$$
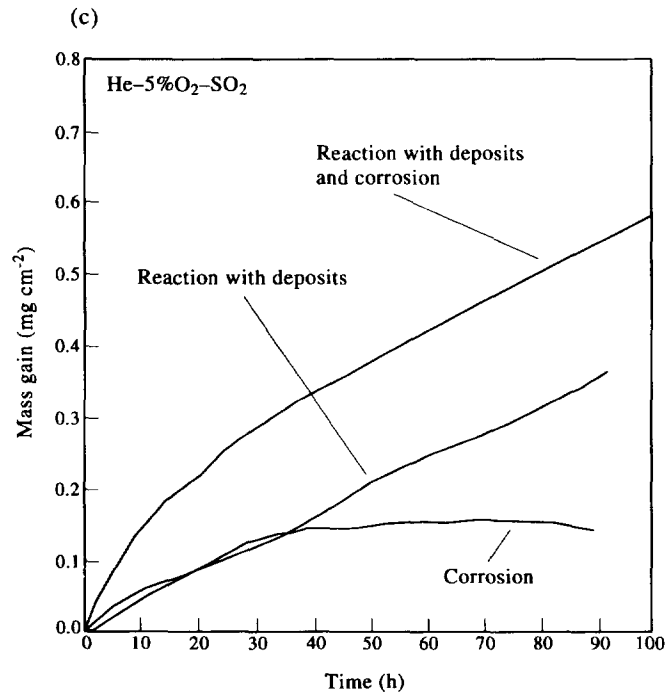
which causes a mass loss. By this reaction a lot of chlorides are generated also at the interface deposit/scale and the interaction of these chlorides with the scale leads to Cl_2-formation and enhanced active oxidation. The conversion of the mixed sulfate to $CaSO_4$ and chlorides has been proven by analysis of the deposit after the experiment (Fig. 11). The SO_2 generated by reaction (12) may also diffuse to the scale/metal interface and causes formation of some FeS which was detected after this experiment. Formation of FeS is also observed below the deposits in power plants.

Finally, the combined effect of SO_2 and HCl in the interaction with the deposit and on the corrosion of the steel beneath deposit and scale was investigated. The mass loss of the deposit caused by HCl is clearly decreased by the presence of SO_2 in the atmosphere (Fig. 12(a)). Obviously, the equilibrium of reaction (12) which would cause mass loss is shifted by the SO_2 to the left hand side, and additionally a sulfation of chlorides takes place, as could be seen from the analysis of the deposit after the exposure according to reaction (11).

The chlorine is generated by these reactions within the deposit, not at the deposit/scale interface, and, thus, most of it diffuses to the atmosphere and only a small part into the scale and to the scale/metal interface. Thus, the active oxidation is much less enhanced in the presence of SO_2 and HCl than in the presence of HCl alone. Increasing the SO_2-addition effectively decreases the mass gain by oxidation (Fig. 12(b)).

(a)

(b)
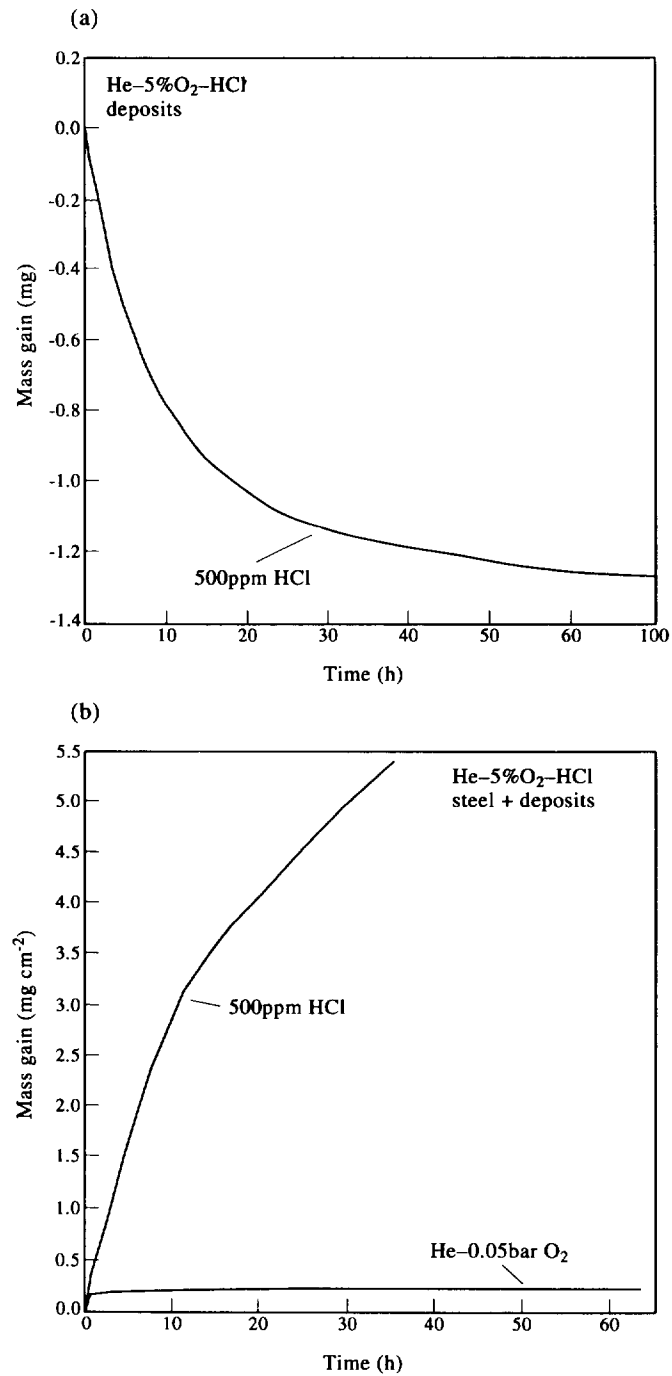
Fig. 10. Effects of HCl on the mass change at 500°C: (a) of only the fly ash by transformation of sulfates to chlorides (reaction (12)); (b) of the steel sample with fly ash deposit, by strongly enhanced active corrosion.

Fig. 11.   SEM micrograph of the deposit after exposure in He–O_2–HCl: crystals of $CaSO_4$
(1) and salt crusts of (K,Na)Cl (2) are observed.

THE CHLORIDE INDUCED ACTIVE OXIDATION OF HIGH ALLOY STEELS

Thermogravimetric studies of the oxidation of some high alloy steels, a 12%CrMoV-steel, a 20Cr–12Ni-steel and a 25Cr–20Ni-steel,[6] were conducted at 700°C as described before, by pre-oxidizing the steels in the horizontal balance for 24 h and then depositing some NaCl on to the oxide scale. As in the case of the low alloy steel an immediate strong acceleration of the mass gain rate was observed (Figs 13(a) and 13(b)), which leveled off after some hours. The oxide scale after such experiments was very loose and porous (Fig. 14) and consisted mainly of Fe_2O_3; the phases $FeCr_2O_4$ and Cr_2O_3 which could be detected after the pre-oxidation were not found (by XRD) after the active oxidation. For these steels this mechanism also applies and the chlorine stems from the reaction of the chloride with the $FeCr_2O_4$ or Cr_2O_3 of the initial scale, according to reaction (3). Also for the steels, the species mainly evaporating is $FeCl_2(g)$, due to its vapour pressure which is higher than that of the chlorides of the other alloying metals. The oxidation of the evaporating $FeCl_2(g)$ leads to the porous unprotective scale of Fe_2O_3.

The 20Cr–12Ni-steel showed, comparatively, very rapid active oxidation. This could be explained by the fact that after pre-oxidation this steel had formed only a very thin oxide layer; the two other steels had an oxide layer about five–six times thicker. The thicker oxide layer has an advantage concerning susceptibility against the chlorine-induced active oxidation, since as has been shown before, the rate controlling process, i.e. the $FeCl_2$-evaporation and diffusion through the scale, is inversely proportional to the thickness of the scale. Thus, in this case a more rapid oxide growth is favourable in obtaining better protection. Usually the alloys are considered as the best ones concerning corrosion resistance on which a very thin, dense layer is growing.

(a)

(b)
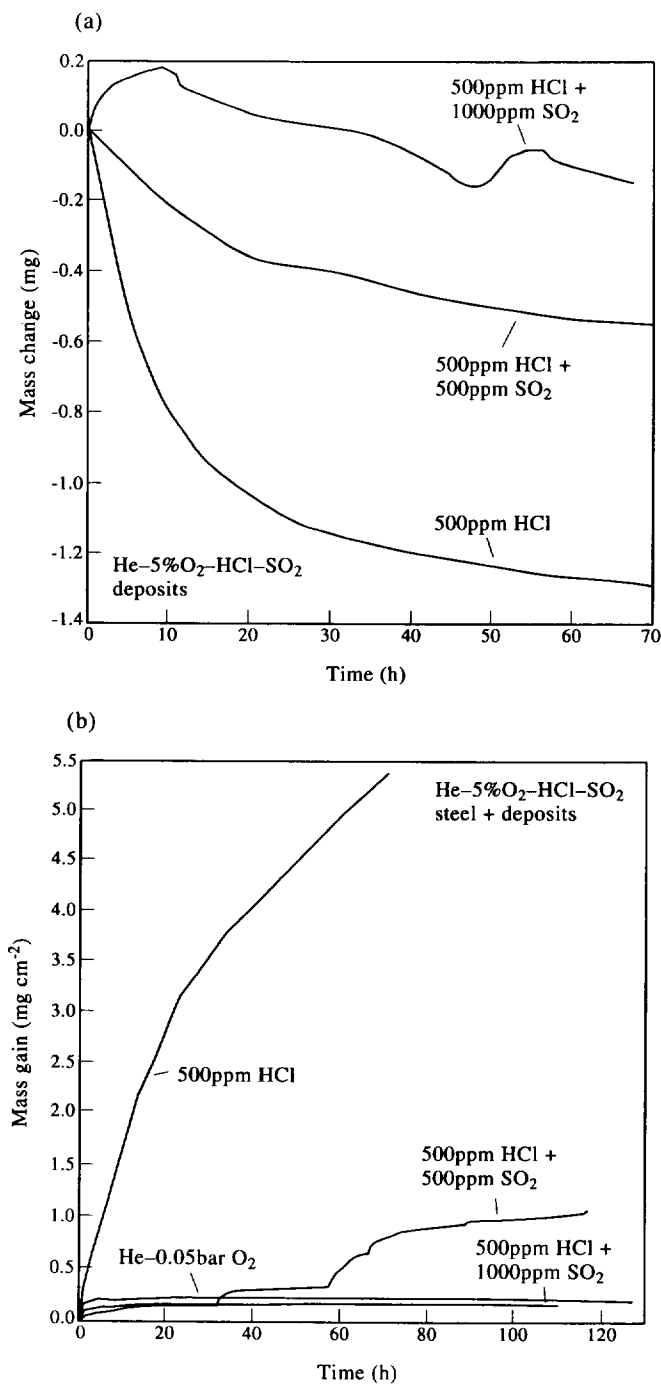
Fig. 12.   Effects of SO_2 and HCl on the mass change at 500°C: (a) of only the fly ash, where sulfation and chlorination come to an equilibrium with not much change; (b) of the steel sample beneath the deposits. where chlorination and active oxidation are increasingly suppressed with increasing SO_2-addition.
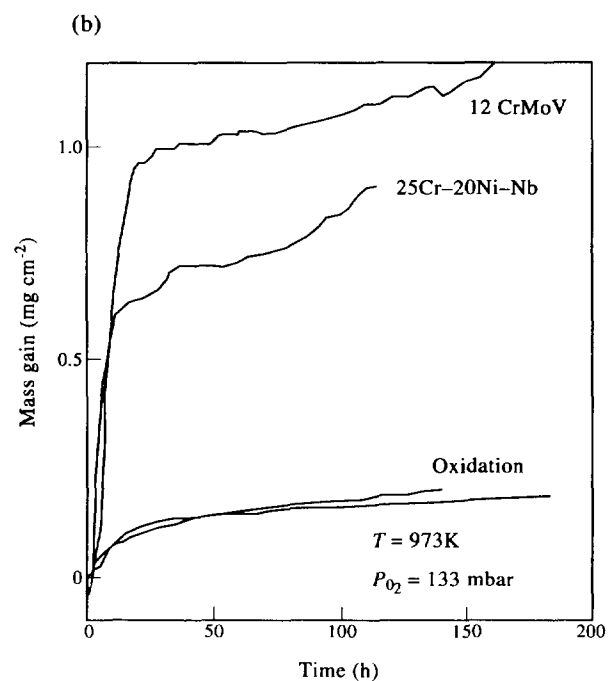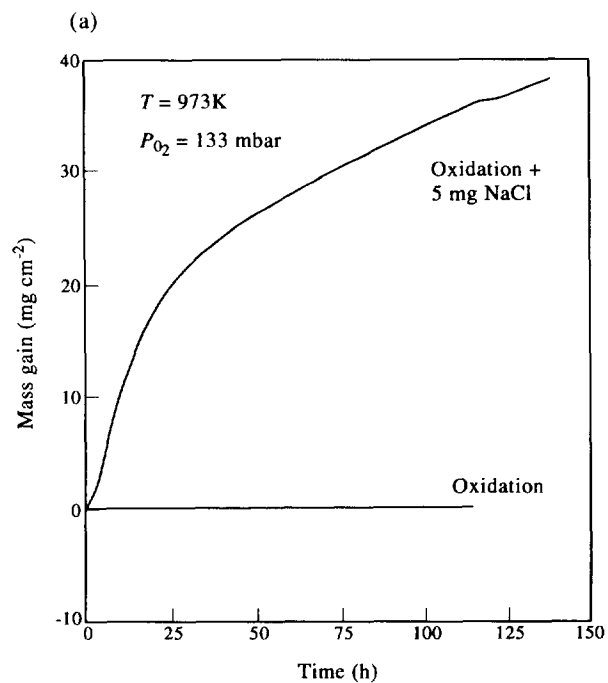
(a)

(b)

Fig. 13.   Mass gain upon oxidation of high alloy steels in He–O_2 at 700°C with and without NaCl deposited after 24 h pre-oxidation as a powder on 0.58 cm^2: (a) of the 20Cr–12Ni-steel; (b) of the 12CrMoV-steel and 25Cr–20Ni-steel.
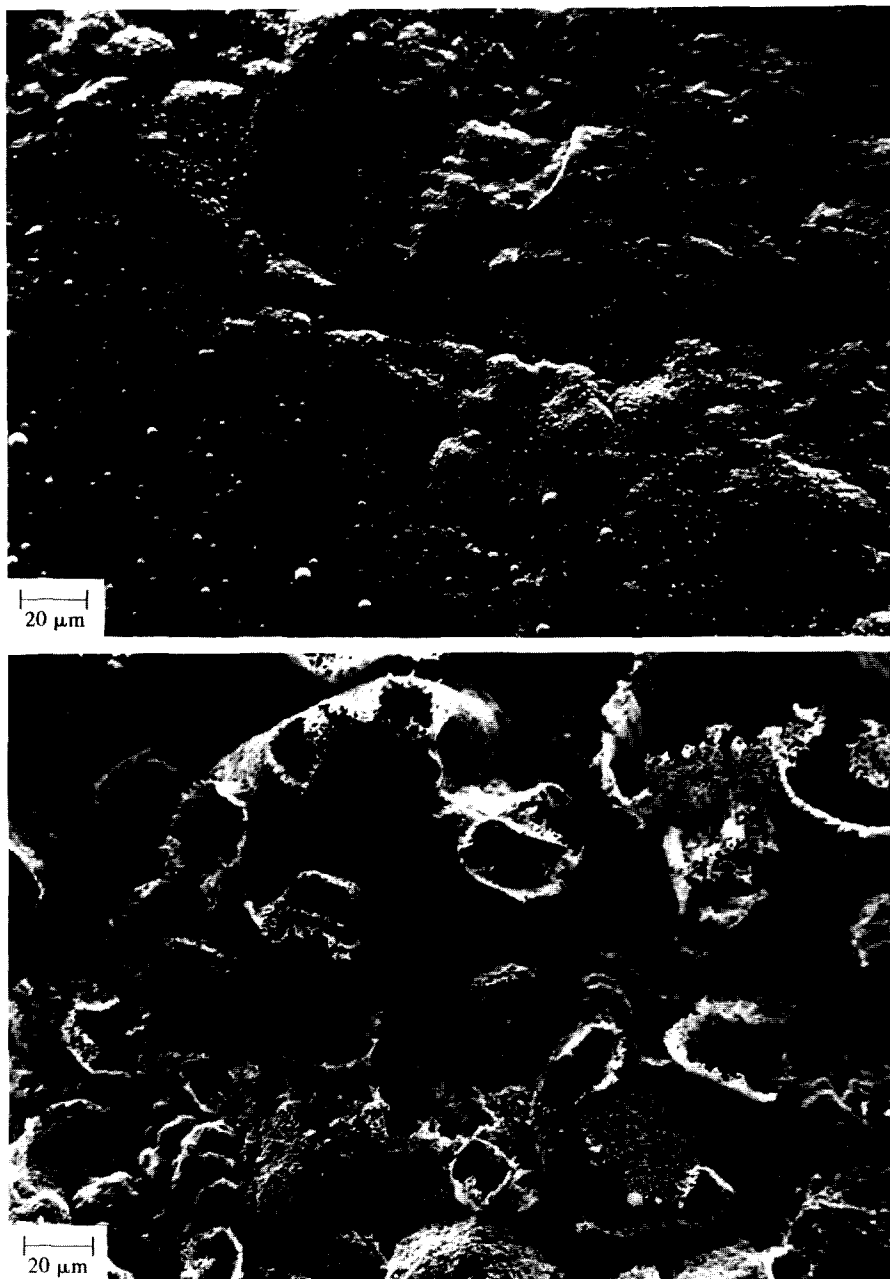
Fig. 14. SEM micrographs (top view) of 12CrMoV steel samples: (a) after oxidation in
He–O_2; (b) after the active oxidation in He–O_2 with NaCl-deposit.

It may be noted that the resistance against chloride induced and accelerated
oxidation is of importance for automotive exhaust systems. In winter salt is strewed
on the streets and may deposit on the hot tubes and mufflers. The 20Cr–12Ni-steel
was used widely and had turned out to be very susceptible. Other steels are now used.

THE CORROSION OF HIGH ALLOY STEELS BENEATH FLY ASH DEPOSITS

Several chromia forming high alloy steels (not all are listed in Table 1) were tested by exposures below deposits at 600°C after a pre-oxidation for 5 h in N_2–O_2, either in N_2–O_2, N_2–O_2–SO_2, N_2–O_2–HCl or N_2–O_2–SO_2–HCl for 360 h.[19] In the pre-oxidation scales of $FeCr_2O_4$ and Cr_2O_3 were formed. After the exposures beneath deposits at 600°C in all cases melts had formed at the deposit/oxide interface, as could be seen by microscopical examination after removal of the deposits. Depending on the presence of SO_2 or HCl in this melt either sulfates or chlorides prevail, and acidic fluxing of the scale is possible, i.e. a dissolution of the chromia under formation of Cr^{3+} ions[20] and the chloride induced active corrosion. The attack in N_2–O_2 beneath deposits led to nearly equal attack of all steels (some basic fluxing by PbO was detected). In the exposures with N_2–O_2–SO_2 a sulfate melt is formed, the formation of SO_3 is catalysed in the deposit and acidic fluxing of the oxide scale can take place, according to

$$Cr_2O_3 + 3\,SO_3 = 2\,Cr^{3+} + 3\,SO_4^{2-}, \qquad (13)$$

$$FeO + SO_3 = Fe^{2+} + SO_4^{2-}, \qquad (14)$$

$$TiO + SO_3 = Ni^{2+} + SO_4^{2-}, \qquad (15)$$
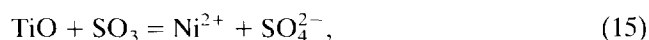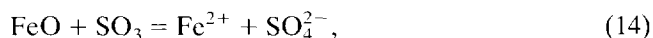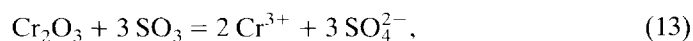
where the reaction equations (14) and (15) are meant for the dissolution of spinels. Since the solubility of Cr_2O_3 in acidic melts is relatively low,[20] the attack is tolerable. The attack beneath the deposits is deleterious in N_2–O_2–HCl. The HCl from the atmosphere transforms the sulfates in the deposit to chlorides, e.g. according to reaction (11). The alkali chlorides and sulfates form a melt which attacks the scales under formation of chromates and chlorine, and the latter initiates the active oxidation. The attack is very severe since molten chlorides are present and can intensely interact with the oxide scale. In contrast, in the exposures in N_2–O_2–HCl–SO_2 the equilibrium of reaction (11) stays at the left hand side, the sulfates remain stable and no chloride containing melt is formed. In this case, acidic fluxing occurs again which is much less deleterious than the active oxidation in the presence of HCl but absence of SO_2.

CONCLUSIONS

In the presence of HCl in the atmosphere, or chlorides as deposits, the oxidation of iron and steel is strongly accelerated. $FeCl_2(s)$ is found at the oxide/metal interface and the loose, porous scale consists of Fe_2O_3. Since the scale is not protective, active oxidation takes place.

The mechanism of active oxidation comprises several steps: the formation of chlorine at the scale surface, penetration of chlorine (or Cl^-) into the scale to the oxide/metal interface, the formation of chlorides of the alloy components—mostly $FeCl_2$ which continuously evaporates and is oxidized to Fe_3O_4—and Fe_2O_3 during its diffusion to the scale surface, forming a non-protective scale. The chlorine returns partially to the scale/metal interface. A reaction circuit exists in which chlorine acts as a catalyst, accelerating the oxidation.

Most striking is the very rapid penetration of the chlorine from the scale surface
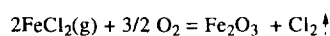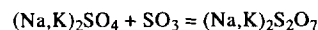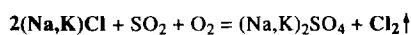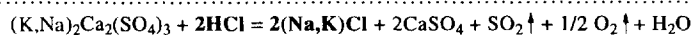
depend on the SO_2 and HCl content of the atmosphere, which determines the sulfate/chloride ratio in this melt. In the case of an oxidizing atmosphere containing only SO_2 (which is oxidized to SO_3) acidic sulfate melts result and the acidic fluxing of chromia scales is minute. In the case of an oxidizing atmosphere containing only HCl, sulfates in the deposit are transformed to chlorides and the contact molten chlorides/oxide scale generates much chlorine, leading to additional detrimental active oxidation.

Surprisingly, for the high alloy steels the situation is less dangerous in the simultaneous presence of SO_2 and HCl, since in the presence of SO_2 the sulfates are stabilized and the chloride induced active oxidation is suppressed. The acidic fluxing of chromia scales is negligible in the temperature range around 600°C.

REFERENCES

1. H. J. Grabke, *Incinerating Municipal and Industrial Waste* (ed. R. W. Bryers), pp. 161–177. Hemisphere Publ. Corp. (1991).
2. D. Bruce and P. Hancock, *J. Inst. Met.* **97**, 140 (1969).
3. P. Hancock, R. C. Hurst and A. R. Sollars, *Chemical Metallurgy of Iron and Steel*, p. 415. The Iron and Steel Inst., London (1973).
4. D. Bramhoff, H. J. Grabke, E. Reese and H.-P. Schmidt, *Werkstoffe u. Korr.* **41**, 303 (1990).
5. E. Reese and H. J. Grabke, *Werkstoffe u. Korr.* **43**, 547 (1992).
6. E. Reese and H. J. Grabke, *Werkstoffe u. Korr.* **44**, 41 (1993).
7. M. J. McNallan, W. W. Liang, S. H. Kim and C. T. Kang, *High Temperature Corrosion* (ed. R. A. Rapp), p. 316. NACE (1983).
8. Y. Y. Lee and M. J. McNallan, *Metallurg. Trans.* **18A**, 1099 (1987).
9. K. Hauffe and J. Hinrichs, *Werkstoffe u. Korr.* **21**, 954 (1979).
10. M. Spiegel and H. J. Grabke, *Werkstoffe u. Korr.* (in press).
11. H. J. Grabke, W. Auer, M. J. Bennett, F. Bregani, F. Gesmundo, D. J. Hall, D. B. Meadowcroft, S. Mrowec, J. F. Norton, W. J. Quadakkers, S. R. J. Saunders and Z. Zurek, *Werkstoffe u. Korr.* **44**, 345 (1993).
12. H. J. Grabke and E. M. Müller, *Werkstoffe u. Korr.* **41**, 226 (1990).
13. J. Robertson and J. E. Forrest, *Corros. Sci.* **32**, 521, 541 (1991).
14. R. J. Fruehan, *Metallurg. Trans.* **3**, 2585 (1972).
15. R. J. Fruehan and L. J. Martonik, *Metallurg. Trans.* **4**, 2789 (1973).
16. J. Halfdanarson and K. Hauffe, *Werkst. u. Korr.* **24**, 8 (1973).
17. K. Reinhold and K. Hauffe, *J. electrochem. Soc.* **124**, 875 (1977).
18. Y. S. Kim and H. W. Pickering, *Metallurg. Trans. B.* **13B**, 349 (1982).
19. M. Spiegel and H. J. Grabke, *Proc. U.K. Corrosion EUROCORR '94*, pp. 307–316. The Chamelion Press Ltd, London (1994).
20. R. A. Rapp, *Corrosion NACE* **42**, 568 (1986).